PSFC/JA-01-6

Edge Ion Heating and Parametric Decay during Injection of Ion Cyclotron Resonance Frequency Power on the Alcator C-Mod Tokamak

J.C. Rost, M. Porkolab, and R.L. Boivin

March 2001

Plasma Science and Fusion Center
Massachusetts Institute of Technology
Cambridge, MA 02139 USA

This work was supported by the U.S. Department of Energy, Contract No. DE-AC02-78ET51013.

Submitted for publication to *Physics of Plasmas*

Edge ion heating and parametric decay during injection of ion cyclotron resonance frequency power on the Alcator C-Mod tokamak

J.C. Rost, M. Porkolab, and R.L. Boivin

March 2001

Abstract

A population of suprathermal ions has been observed in the scrape-off layer during injection of power in the ion cyclotron frequency range on the Alcator C-Mod tokamak. These ions generated energetic neutrals measured with a charge-exchange neutral particle analyzer. In the hydrogen minority heating regime, fast particles were generated only when the injected power was above 500 kW. Fast particles were observed at a low level of injected power when the frequency was a multiple of the ion cyclotron frequency in the scrape-off layer. The power deposited in the edge was always less than a few percent of the injected power and did not increase impurity levels. The theoretical threshold of parametric decay instabilities for decay of the pump wave in the antenna near field into an ion Bernstein wave and an ion cyclotron quasimode matches the observed threshold for fast ion production under a variety of conditions.

1 Introduction

The production of fast ions ($\mathcal{E} > 5$ keV) in the scrape-off layer (SOL) was observed regularly during the injection of rf power in the ion cyclotron resonance frequency (ICRF) range on the Alcator C-Mod tokamak.[1] This phenomenon was studied using a passive charge-exchange neutral particle analyzer (NPA).

The threshold in rf power for edge ion heating depends strongly on the magnetic field. During hydrogen minority heating at the center, with the toroidal field B_0 at 5.3 T, edge ion heating occurs only during high power rf heating, $P_{\rm rf} > 0.5$ MW, and the percentage of the incident rf power absorbed by the edge is much less than 1%. However, at values of B_0 such that the rf frequency is at an ion-cyclotron harmonic in the edge, $\omega_{\rm rf} = \ell\omega_{\rm cD}({\rm edge}), \ell = 3, 4\ldots$, edge ion heating occurs at very low rf power, less than 10 kW. The rf power absorbed directly by the plasma edge in such cases can be up to 5% of the incident power. The level of edge heating depends on edge plasma conditions and increases significantly during ELM-free H-modes. The edge ion heating on Alcator C-Mod has no detrimental effect on the plasma performance; it does not lead to increased impurity production or reduce the coupling between the rf antennas and the plasma.

Parametric decay into an ion Bernstein wave and an ion cyclotron quasimode couples power to ions and can cause the ion edge heating observed.[2] Also, rf probe spectra typical of parametric decay instabilities (PDI) have been observed on Alcator C-Mod.[3]

The theory of PDI in a uniform plasma was used to calculate the threshold for convective instability of the most unstable mode in terms of plasma density and temperature, magnetic field, and amplitude of the rf electric field. The calculated threshold matches the observed threshold for ion tail generation in the SOL, including the strong dependence on B_0. Furthermore, the observed difference between heating of H and D ions at different harmonics is predicted as well.

Edge ion heating during ICRF heating can potentially harm plasma performance in several ways. Coupling of rf power from the antenna through the plasma edge to the bulk plasma can be strongly affected by the edge conditions.[4] Also, the rf power absorbed directly by the plasma edge reduces the power available for central heating or current drive. The unconfined fast ions can contribute to impurity generation; significant impurity generation has been linked to edge ion heating, as described below. Furthermore, various enhanced confinement modes that depend on edge conditions could be affected.

Generation of energetic edge ions has been observed during ICRF fast wave heating on several tokamaks, including ASDEX, JT-60, and TEXTOR. Here we summarize the techniques used in each case for the detection of fast ions, the operating parameters, and the evidence of PDI for comparison with our observations on Alcator C-Mod. Edge heating and parasitic power loss in other rf heating regimes, e.g. due to parametric decay of lower hybrid waves,[5] are separate topics by virtue of the differences in power density, wave structure, and launching techniques and are not considered here.

During the ASDEX experiments ($B_0 = 2.2$ T, $P_{\rm rf} = 1.2$ MW, rf = 67 MHz, $R_0 = 1.67$ m, $a = 0.40$ m, $\bar{n}_e = 2 - 6 \times 10^{19}$ m^{-3}, double null) deuterons with large perpendicular velocities were observed when an antenna with an optically-open Faraday screen was used.[6]

The deuterium flux, measured with a charge-exchange analyzer, showed fast rise and decay times, 1–3 ms, and was very sensitive to toroidal field, leading them to conclude that the flux originated in the plasma edge. Measurements made with carbon implantation probes showed fast deuterium ions up to 15 keV striking the probe in the rf antenna.[7] Parametric decay was observed with rf probes, but not compared with the NPA measurements.[8] PDI was only seen at certain magnetic fields.

Investigations of edge effects during ICRF heating on TEXTOR ($B_0 = 2.2 - 2.6$ T, $P_{\rm rf} = 1.6$ MW, rf = 29 MHz, $R_0 = 1.75$ m, $a = 0.45$ m, $\bar{n}_e = 6 \times 10^{19}$ m^{-3}, limited, circular) showed the presence of fast ions in the SOL.[9] Measurements using laser induced fluorescence with sputtered Fe atoms determined qualitatively that a population of fast ions existed in the SOL. The sputtering yield increased quickly, in less than 1 ms, compared to time scales for changes in the power flux to the limiters or the bulk plasma parameters ($\sim$ 100 ms). Measured increases in SOL density and temperature did not account for the observed increases in sputtering and heat flux to the divertor.

Fast ions were observed on the JT-60 tokamak with charge-exchange analyzers during second-harmonic hydrogen minority heating ($B_0 = 3.7 - 4.3$ T, $P_{\rm rf} = 1.5$ MW, rf = 110 − 130 MHz, $R_0 = 3$ m, $a = 0.93$ m, outboard diverted).[10] The charge-exchange analyzer measuring the flux of neutrals with energies of 3.9 keV and 5.6 keV observed a flux "jump" with the injection of ICRH when the antennas were operated with (0,0) phasing, but not when the antennas were operated with (0,π) phasing. Note that (0,0) phasing generally results in larger electric fields near the antennas. RF probes concurrently observed parametric decay into an ion cyclotron quasimode and an ion Bernstein wave. The IBW amplitude and the jump in flux were found to be positively correlated during a toroidal field scan, leading them to conclude that the parametric decay generated the energetic ions. Radiation losses from the plasma were also correlated with IBW amplitude, implying that the PDI led to increased impurities in the plasma.

The main content of this paper is divided into two main sections. Section 2 describes the measurements and experiments performed on C-Mod. Section 3 describes the method and results of the PDI threshold calculations and compares them to the observations.

2 Observations of edge ion heating on Alcator C-Mod

The edge ion heating experiments described below were performed on the Alcator C-Mod tokamak at the Massachusetts Institute of Technology Plasma Science and Fusion Center. The effect is characterized by the observations made with a scanning charge-exchange neutral particle analyzer (NPA).

Note that the effect here referred to as "edge ion heating" is, more strictly speaking, suprathermal tails in the ion distribution function perpendicular to the magnetic field. The tails are located on open field lines in the SOL. There is no change in the bulk ion temperature in the SOL. Furthermore, while the NPA measures escaping neutrals, the source of these neutrals is unambiguously charge-exchange between neutrals and plasma ions and we speak of the diagnostic as measuring the plasma ions.

We precede the details of this study with a brief description of Alcator C-Mod and the analysis of charge-exchange neutrals.

2.1 Plasma parameters and diagnostics

Alcator C-Mod is a compact, high-field tokamak: $R_0 = 0.67$ m, $a = 0.22$ m, $B_0 < 9$ T.[1] The experiments described herein exploit only a small part of the wide range of plasma parameters and rf heating scenarios[11] that have been used.

At the time of this study, the rf system consisted of two double-strap antennas with Faraday shields which heat the plasma by launching a fast wave at 80 MHz with delivered power up to 3.5 MW. The antennas have protection limiters on the sides that extend out 5 mm radially.

Edge ion heating observations made during hydrogen minority heating had $B_0 = 5.3$ T, $I_p = 800$ kA, $T_e = 1 - 4$ keV, $T_i = 1 - 3$ keV, $[H]/[D] \leq 10\%$. The rf power damps strongly on hydrogen in the plasma center, where $\omega_{\rm rf} = \omega_{\rm cH}$. The effect of the magnetic field on edge heating was explored with $B_0 = 2.6 - 4.8$ T, $I_p = 550 - 800$ kA, $\bar{n}_e \sim 2 \times 10^{20}$ m^{-3}, where no significant damping of the rf waves on the bulk plasma is expected.

Plasma parameters outside the LCFS are found to have a large effect on edge heating. On Alcator C-Mod, measurements with a fast scanning probe (FSP) show the presence of significant plasma at the outboard RF limiter radius with $n_e \geq 1 \times 10^{19}$ m^{-3}, $T_e = 10 - 20$ eV.[12] At this distance from the LCFS, the ion temperature is unknown, but is believed to excede the dissociation energy of the hydrogen molecule, $T_i \gtrsim 3$ eV. We note in advance that the parametric decay thresholds we calculate depend sensitively on these values.

Neutral particle analyzer

All particle measurements described here were made using a passive charge-exchange neutral particle analyzer. The basic function of the NPA is to count the number of incoming energetic neutral hydrogen and deuterium atoms at various energies. The source of these neutrals is charge-exchange reactions in the plasma. Using the appropriate calibration factors and cross section, the integral along the sightline of the ion distribution function is obtained,

$$\hat{f}(v) = \int dl f_i(\mathbf{v} = v\mathbf{l}, \mathbf{x}) n_0(\mathbf{x}) e^{-\int \alpha dx'}, \tag{1}$$

where $\mathbf{l}$ is the unit vector along the sightline at $\mathbf{x}$, α represents attenuation, primarily due to reionization of escaping neutrals or another charge exchange, and n_0 is the density of neutral hydrogen.

If the only significant source of energetic neutrals is ion tails in the plasma edge, Eq. 1 can be written as

$$\hat{f}(v) \simeq f_i(\mathbf{v} = v\mathbf{l}, \text{edge}) n_0(\text{edge}) \Delta x. \tag{2}$$

The NPA on Alcator C-Mod used in these studies is the $E \parallel B$ type.[13, 14] Hydrogen and deuterium fluxes are measured simultaneously. Microchannel plates are used for particle

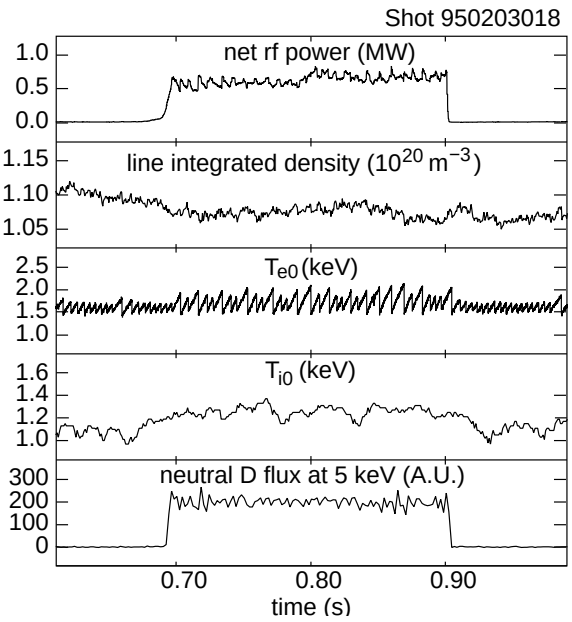

Figure 1: Time trace of plasma signals showing jump in neutral particle flux indicative of edge heating. Ion temperature is obtained from the neutron production rate.

detection, with 39 energy channels for each species. The most common energy range used is 0.5–20 keV for deuterons. Species contamination between the H and D rows and rf pickup were negligible, and random detector noise is monitored and accounted for. The time response is primarily limited by the need to acquire a sufficient number of counts per time bin. Usually, time bins were set at 2 ms, but edge ion heating was measured with time bins as short as 0.1 ms.

The "home" position of the NPA is perpendicular to B_0 and horizontal through the midplane. The NPA is physically scanned between shots either poloidally or toroidally, pivoting about a point on the midplane at $R = 2$ m. The extreme sightline in toroidal scans is tangent at $R = 0.41$ m. Scanning poloidally, the height which the NPA sightline passes through R_0 ranges between $z = -.25$ and 0 m.

The NPA was in the port next to the rf antennas, approximately 36° away toroidally.

2.2 Observations of energetic neutral flux

Edge ion heating on C-Mod is identified primarily by a large, sudden increase in the flux of energetic neutral hydrogen or deuterium atoms as shown in Fig. 1. The extra flux is observable between a minimum energy around 1 keV, below which the flux does not change, and a maximum of $20 - 50$ keV where the signal becomes too small to be resolved above the noise. In this range, the magnitude of the increase varies significantly, up to three orders of magnitude.

2.2.1 Location of the fast ions

Because critical parameters including the density, temperature, confinement time, neutral density, and rf field magnitude can vary by orders of magnitude over the distance of a few centimeters, the location of the fast ions in the plasma must be determined before their effect and possible source can be assessed. Several characteristics of the increase in neutral flux during ICRF injection indicate that the source of fast neutrals is charge exchange of fast ions in the plasma edge: the time scale of the change is fast, the neutron production rate remains unchanged while the ion tails are observed, and the threshold is sensitive to edge parameters. These criteria are those generally used in the previous works cited above.

The jump in neutral flux occurs on time scales too short to be resolved by the analyzer, which was generally operated with 2 ms time bins. Even on occasions when the time base was decreased to 0.1 ms the jump could not be resolved. This time is much faster than time scales for increases in density or ion temperature in the core plasma, which are slower than 10 ms.

If the fast ions were located inside the bulk plasma, the neutron production rate from D-D reactions would have shown the same sharp increase as the neutral flux. The cross-section for D-D reactions has a strong energy dependence, so this measurement is quite sensitive to fast ions. However as in Fig. 1 no increase has been seen. As the dependence on neutral density and the attenuation of charge-exchange neutrals makes the NPA effectively 3–5 orders of magnitude more sensitive to ions in the plasma edge, the level of fast neutrals measured would correspond to a small population of fast ions in the edge or a large population in the plasma center. The constant neutron rate therefore implies that the fast ions are located in the plasma edge.

Edge heating is not seen on every shot with rf power. Whether or not it occurs on a given shot depends on the edge conditions. As will be described more fully below, enhanced neutral flux is observed at much lower rf power levels when B_0 was set so that $\omega_{\rm rf} = \ell\omega_{\rm cD}$ in the SOL at the outboard midplane and is sensitive to changes in B_0 as small as 1%.

The jump in neutral flux is sensitive to the changes in the edge conditions that occur at the transition to ELM-free H-mode, either from ELM-y H-mode or L-mode as shown in Fig. 2. As described in Section 3 of this paper, the critical change in plasma parameters at the transition is a decrease in ion temperature in the outer SOL. Notably, the previous studies of edge ion heating cited above do not contain any data related to H-mode.

2.2.2 Edge heating during hydrogen minority heating

During hydrogen minority heating in a deuterium plasma, edge ion heating is observed with the NPA only at rf power levels above approximately 500 kW. When the threshold is exceeded, the magnitude of the edge heating does not otherwise depend on the rf power level.

Plasma shots with a wide range of parameters were examined to search for the threshold for edge heating. We found that there is no threshold in the total injected rf power; i.e. operating both antennas at 250 kW each did not generate fast ions, while operating the E-

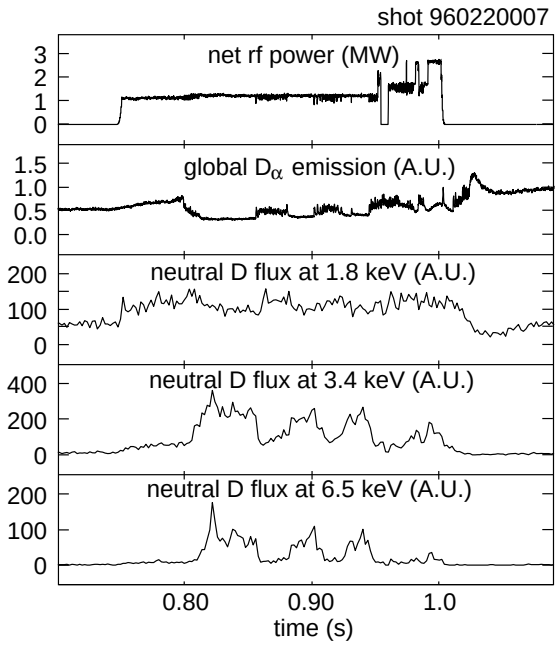

Figure 2: The level of energetic neutral flux due to edge heating increases during ELM-free H-mode. This discharge exhibits several transitions from ELM-free to ELM-y H-mode.

port antenna at 500 kW did. There is however a threshold in rf antenna voltage; a necessary condition for edge ion heating is that at least one antenna be operating at a voltage of ~ 20 kV, as shown in Fig. 3. There are many shots over this threshold where edge heating is not observed. The poloidal electric field of the antenna is continuous from inside the current strap to the region immediately outside it. From this we estimate that an rf voltage of 20 kV on the current strap generates a near field in the poloidal direction of roughly 100 kV/m. This evanescent field, which is due to the self-inductance of the antenna and is unrelated to the coupled power, exists only within a few cm of the current strap. The electric field component of the propagating fast wave coupled to the plasma in such a case is estimated to be 12 kV/m.

This important observation indicates that the edge ion heating is caused directly by the rf near field of the antennas. If the energetic neutral flux were a byproduct of linear absorption of the rf waves in either the edge or the core, the effect of the two antennas would be additive in power. The threshold in local rf electric field suggests that a nonlinear process is at work.

For plasma shots above the threshold, the presence or absence of edge heating was not correlated with any bulk plasma parameter. The PDI threshold calculations suggest that the ions are generated in the outer SOL; far out in the SOL, the density and temperature may not be strongly correlated with the bulk plasma parameters as they are near the LCFS.

There are plasma discharges in which edge heating starts at the L–H transition, after the start of ICRH. This also suggests that the threshold depends on the edge plasma parameters.

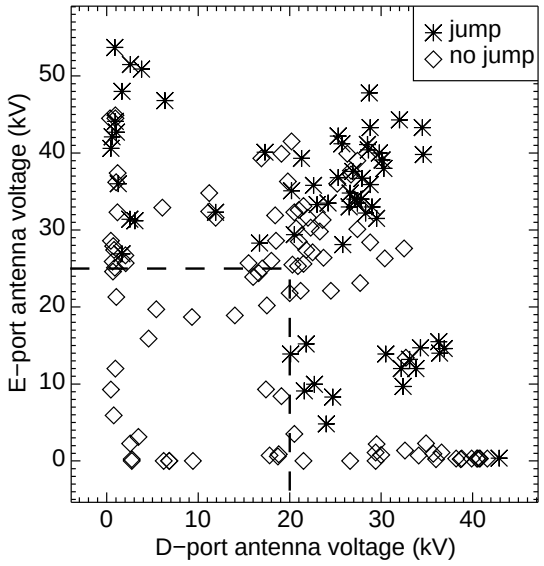

Figure 3: Edge heating is observed when the rf antenna voltage on either antenna is greater than 20 kV. Each symbol represents a single plasma discharge; stars represent discharges where the energetic neutral flux "jumped" when rf power was applied, indicating edge heating.

2.2.3 Edge heating with rf at resonance in the SOL

The edge ion heating behavior is distinctly different from that observed during hydrogen minority heating when $\omega_{\rm rf} = \ell\omega_{\rm cD}$ near the LCFS, $\ell = 3, 4, 5, 6, 7$ (no data for cases with $\ell > 7$ was obtained). Harmonics do not occur in the SOL for values of B_0 used in the C-Mod ICRF heating scenarios. However, this range of $\omega_{\rm rf}/\omega_{\rm cD}$ may be relevant to high harmonic fast wave current drive studies.

At these fields, the threshold for edge heating is very low, below 10 kW. Edge ion heating may occur predominantly for hydrogen or deuterium, depending on the harmonic number ℓ, as shown in Fig. 4. This is further evidence that the ion tails are being generated by a non-linear wave-particle interaction, not a global plasma effect.

Edge ion heating is restricted to the local region of the SOL where $\omega_{\rm rf} \simeq \ell\omega_{\rm cD}$. This is confirmed by measurements made during a NPA scan at several vertically spaced sightlines with the toroidal field ramping, as shown in Fig. 5. As the toroidal field is ramped, the cyclotron harmonic $\omega_{\rm rf} = \ell\omega_{\rm cD}$ is swept through the plasma. The bursts of neutral particles occur only when the harmonic is in SOL in the NPA sightline. This plot indicates that ions with large perpendicular energies are generated only in the volume of the SOL where $\omega_{\rm rf} \simeq \ell\omega_{\rm cD}$ locally. The x-axis for each sightline is corrected for poloidal field, toroidal field ripple, and the NPA sightline angle to show the radius of the banana tips ($v_\parallel = 0$) of the particles observed.

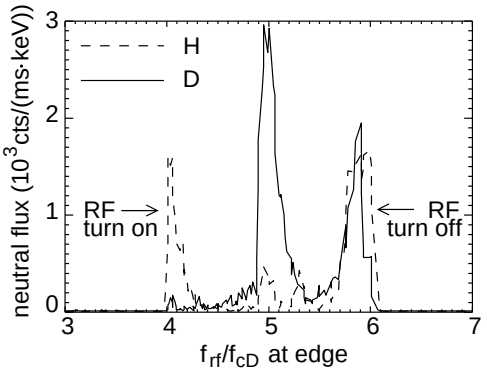

Figure 4: Hydrogen and deuterium flux at 4.85 keV shows edge heating occurring at low power when rf is at a cyclotron harmonic in the edge. Plasma has $\sim 10\%$ hydrogen. Data comes from a single shot in which B_0 ramps, effectively moving different resonances through the edge.

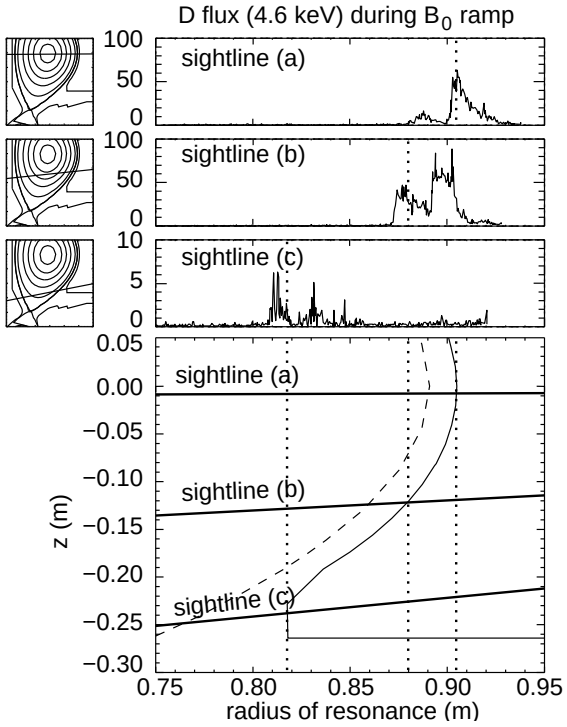

Figure 5: Neutral flux measurements at multiple poloidal sightlines during a B_0 ramp show that edge heating is radially and poloidally localized in the volume of the SOL where $\omega_{\rm rf} \simeq \ell\omega_{\rm cD}$.

2.2.4 Impurity production and rf loading

In experiments on Alcator C-Mod, edge ion heating does not increase impurity production or affect the loading of the rf antennas. This is in specific contrast to JT-60 results that observed a correlation between edge heating via PDI and impurity levels.[10]

To examine this issue, the toroidal field was ramped, moving a resonance through the edge, with constant rf power. No increase in radiated power or molybdenum levels was seen when the edge ion heating started. Similarly, no effect on the rf antenna loading was seen.

2.2.5 Power deposition in the edge

Because of the importance of parasitic absorption of the rf power in the plasma edge, we present details of the assumptions and scalings used to form this estimate. To estimate an upper limit on the maximum power being absorbed by edge ions, a toroidal scan of the NPA was made with $\omega_{\rm rf} \simeq 3\omega_{\rm cD}$(edge) and 500 kW of rf power. Energetic neutral flux was significant only within 20° of perpendicular. Because these particles have large banana widths and Larmor radii, we made the assumption that they would be scraped off by the rf protection limiters on their first orbit, resulting in a confinement time roughly 1/4 of a bounce period. Because the bounce period is shorter than the mean time to charge exchange, the power going into edge ions is much more than the power observed as escaping energetic neutral flux, $P_{\rm edge} = (\tau_{\rm cx}/\tau_{\rm bounce})P_{\rm neut}$. Because the neutral density in the edge is unknown, a scale factor for the NPA signal is calculated during the ohmic part of the shot based on profiles from other diagnostics and applied to the power flux during ICRF injection. We assume that the edge heating is toroidally symmetric because the rf power is far above threshold for this value of B_0. Integrating over pitch angle, plasma surface, and particle energy, we find that the power into edge ions is approximately 5% on these shots. Note that this case was chosen specifically to provide an upper limit. During hydrogen minority heating, however, the level of edge heating is lower even at higher rf power, and is expected to be localized near the antennas, leading to a parasitic loss of $\ll 1\%$. Furthermore, two assumptions made, namely that the neutral density is constant over the SOL and that all the fast edge ions are on orbits intersecting a material surface, make the estimate an upper limit. More realistic modeling would decrease the estimate of parasitic power loss.

While a 5% loss in heating power would not significantly affect the heating efficiency of an ICRF heating system, the deposition of 5% of the injected power onto a small area of the vacuum vessel in the form of energetic ions could have important consequences, such as significant sputtering and impurity generation.

3 Parametric Decay Instability in the ICRF Range

As described above, several observations suggest that a nonlinear wave-particle interaction near the rf antennas generates the fast ions observed in the SOL on Alcator C-Mod. In this half of the paper, we describe the calculation of the threshold for one type of parametric

decay instability (PDI) and show that the observed thresholds under various conditions are reproduced.

Parametric decay instabilities in plasmas generally cause the decay of a pump wave into two daughter waves or modes via nonlinear coupling. The modes must obey the conservation equations

$$\omega_1 + \omega_2 = \omega_0 \quad \text{and} \quad \mathbf{k}_1 + \mathbf{k}_2 = \mathbf{k}_0. \tag{3}$$

PDI has been observed in several types of tokamak rf heating: fast wave,[8, 10] ion Bernstein wave,[15] and lower hybrid.[5]

At the frequencies used for fast wave heating, the rf pump wave can decay into an ion Bernstein wave and an ion-cyclotron or electron quasimode.[2] The IBWs involved in the decay have $k_\parallel \neq 0$, and the waves may propagate at any angle with respect to the magnetic field. Ion cyclotron quasimodes are not propagating waves, rather they represent large density fluctuations at frequencies $\omega = \ell\omega_{ci}$ that exist only in the presence of the pump wave. Ion cyclotron quasimodes damp efficiently on cold ions and could generate the fast ions observed in the SOL. Whereas propagating waves are described by the solution of the dispersion relation $\epsilon = 0$, for ion cyclotron quasimodes $\epsilon \simeq i\,\mathrm{Im}(\chi_i) \gg 1$. The fact that χ_i is large and imaginary implies that the fluid current is in phase with the electric field, so the power deposited on the ions $P = \langle \mathbf{E} \cdot \mathbf{j} \rangle$ is large.

3.1 Linear growth rate of parametric decay instabilities

The growth rates for parametric decay instability are calculated assuming that the plasma is uniform and magnetized and the pump wave is spatially uniform.

The equation describing the growth rate of the parametric decay instability in the ICRF regime is derived from a Vlasov equation by including the pump wave to lowest order, leading to coupling of modes related as in Eq. 3 and a dispersion relation[16]

$$\epsilon(\omega_1)\epsilon(\omega_2) = -\frac{1}{8}\sum_{\sigma,\nu} |\mu_\sigma - \mu_\nu|^2 \big[\chi_\sigma(\omega_1) - \chi_\sigma(\omega_2)\big]\big[\chi_\nu(\omega_1) - \chi_\nu(\omega_2)\big]. \tag{4}$$

The sums over ν and σ are over species in the plasma. The χ's are defined as the standard hot plasma susceptibilities. The coefficient μ, which must satisfy $\mu \ll 1$, is a coupling coefficient related to the quiver velocity in the rf electric field,

$$\mu_\sigma = \frac{q_\sigma}{m_\sigma}\left[\left(\frac{\mathbf{E}_\perp \cdot \mathbf{k}_\perp}{\omega_0^2 - \omega_{c\sigma}^2} + \frac{E_\parallel k_\parallel}{\omega_0^2}\right)^2 + \frac{|\mathbf{E}_\perp \times \mathbf{k}_\perp|^2 \omega_{c\sigma}^2}{(\omega_0^2 - \omega_{c\sigma}^2)^2 \omega_0^2}\right]^{1/2}, \tag{5}$$

where $E_\parallel$ and $\mathbf{E}_\perp$ refer to the components of the pump wave parallel and perpendicular to the magnetic field, respectively.

With the usual assumptions of small growth rate and identifying the real parts of ω_1 and ω_2 with the quasimode frequency ω_{ICQM} and the IBW frequency ω_{IBW}, Eq. 4 can be solved

for the growth rate,[2]

$$\gamma \simeq \left(\frac{\partial \epsilon_R}{\partial \omega_{\rm IBW}}\right)^{-1} \left\{ -\epsilon_I(\omega_{\rm IBW}) + \sum_{\sigma,\nu} \frac{|\mu_\sigma - \mu_\nu|^2}{4} \,{\rm Im}\left[\frac{(\chi_\sigma(\omega_{\rm ICQM}) - \chi_\sigma(\omega_{\rm IBW}))(\chi_\nu(\omega_{\rm ICQM}) - \chi_\nu(\omega_{\rm IBW}))}{\epsilon(\omega_{\rm ICQM})}\right]\right\}. \quad (6)$$

The solution to $\epsilon_R(\omega_{\rm IBW}) \simeq 0$ describes the ion Bernstein wave, and so $-\epsilon_I/\frac{\partial \epsilon_R}{\partial \omega}$ in Eq. 6 describes the linear damping of the IBW. The term proportional to μ^2 is the PDI driving term. It must be larger than the IBW damping term for the decay modes to grow.

Collisional damping can be neglected in cases where $\nu_{ei} \ll \omega_{\rm IBW}$, as it is under our conditions.

3.2 Numerical calculations and comparison to experiment

The threshold for instability is defined as the electric field sufficient for an initial perturbation to grow significantly as it passes through the decay region, $\gamma L/v_g > \pi$, by convention. In practice, the growth rate γ and the group velocity $\mathbf{v}_g$ can vary significantly across the SOL, although the scale lengths are much longer than the wavelength of the decay waves. We use $\mathbf{v}_g$ to calculate the trajectory $x(t)$ of the perturbation across the pump region, including the refraction and the spatial variation of $\mathbf{k}$. Using the uniform growth rate γ calculated at points along the trajectory, the convective growth is estimated as $\int \gamma(x(t))dt$. Only the radial and toroidal directions need be considered because the poloidally propagating perturbations are strongly refracted in the radial direction by the parameter gradients. The toroidal extent of the pump wave is 0.5 m, the width of the rf antenna. The effective radial width of the growth region is about 5-20 mm.

Growth of the PDI is examined for the two regimes of interest where edge heating is observed. For hydrogen minority ICRH, we find that the electric field threshold in the outer SOL matches the threshold in the antenna near field for edge ion heating to be observed. When B_0 is such that $\omega_{\rm rf} \simeq \ell\omega_{\rm cD}$ in the edge, the convective growth is very high even at low rf power levels.

3.2.1 Minority heating regime

During hydrogen minority heating in Alcator C-Mod, $\omega_{\rm rf} = 2.7\omega_{\rm cD}$ in the SOL. The pump wave decays into an ion cyclotron quasimode at $\omega_{\rm cD}$ and an IBW at $1.7\omega_{\rm cD}$. At that frequency, $k_\perp \rho \sim 1$ for the IBW. In finding the threshold, $k_\parallel$ is varied to maximize the convective growth. For the parameters used, the maximum convective growth occurs for $k_\parallel$ in the range of 50 to 100 m^{-1}.

If $T_e = T_i$ at the appropriate n_e, the strongest decay is into an electron quasimode at $\omega \lesssim \omega_{\rm cD}$ and an IBW. This does not lead to ion heating. When $T_e > T_i$, however, decay involving the ion cyclotron quasimode dominates. This suggests the picture that

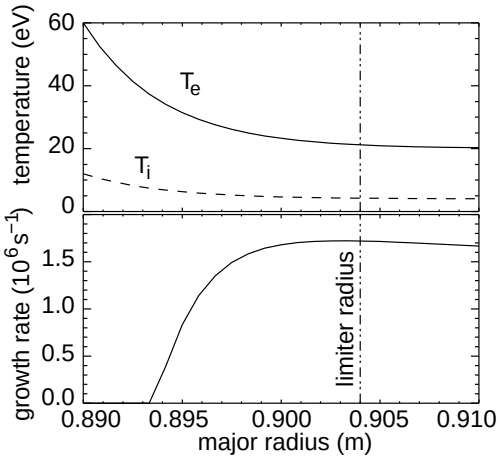

Figure 6: Temperature profiles and PDI growth rate from the LCFS to the antenna limiter. Electron temperature profile represents a typical case, while ion temperature profile is assumed.

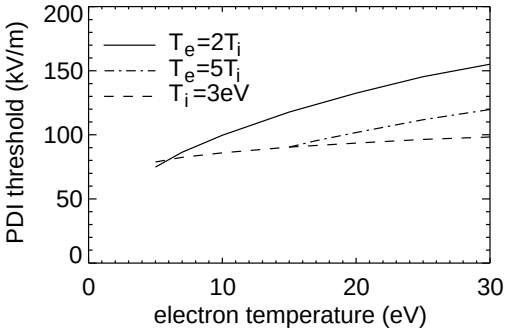

Figure 7: PDI threshold rf electric field as a function of plasma temperature.

$T_e \sim 10 - 20$ eV as measured by the fast scanning probe, and $T_i \gtrsim 3$ eV, the hydrogen dissociation energy per atom.

Keeping terms significant for decay into an ICQM, Eq. 6 can be rewritten as

$$\gamma \simeq \left(\frac{\partial \epsilon_R}{\partial \omega_{\mathrm{IBW}}}\right)^{-1} \left(-\operatorname{Im}\chi_e(\omega_{\mathrm{IBW}}) + \frac{|\mu_D|^2}{4}\operatorname{Im}\chi_e(\omega_{\mathrm{ICQM}})\right). \tag{7}$$

Because the IBW frequency is only 1.7 times the quasimode frequency, the IBW damping, which is proportional to $\operatorname{Im}\chi_e(\omega_{\mathrm{IBW}})$, will be significant whenever the growth term, which is proportional to $\operatorname{Im}\chi_e(\omega_{\mathrm{ICQM}})$, is significant. This accounts for the relatively high electric field threshold for these ICRH discharges.

Figure 6 shows the dependence of the growth rate on radius in the SOL for one set of parameters near the threshold. PDI threshold as a function of temperature is shown in Fig. 7. It is clear immediately that parametric decay will only occur at temperatures found in the outer SOL, and then only at the rf electric field magnitudes found in the near field of the

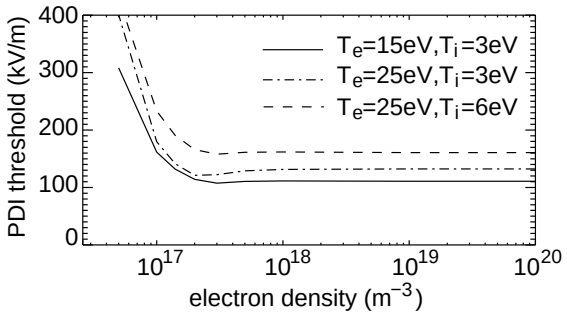

Figure 8: PDI threshold rf electric field as a function of plasma density.

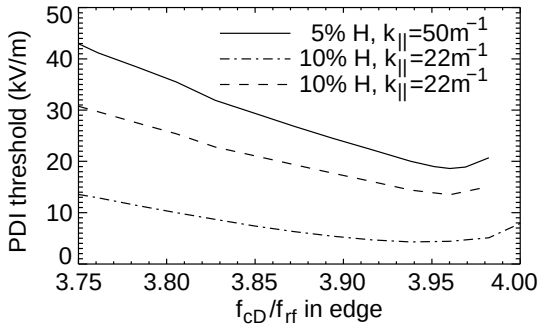

Figure 9: PDI threshold electric field depends strongly on the ratio of $f_{\rm rf}/f_{\rm cD}$ when the rf is near a cyclotron resonance. Calculations for this plot used $k_\parallel$ of 20 and 50 m^{-1}, SOL temperatures of $T_e = 20$ eV and $T_i = 5$ eV, and hydrogen concentrations of 5% and 10%.

C-Mod antennas. The experimentally observed threshold for edge ion heating occurs when the poloidal electric field near the antenna is approximately 100 kV/m. This approximately matches the calculated PDI threshold at $T_e = 20$ eV, $T_i = 4$ eV.

This result explains the soft lower threshold shown in Fig. 3. The hydrogen dissociation energy of 3 eV is a minimum possible ion temperature, but not a maximum. This suggests the hypothesis that discharges which showed edge ion heating at an rf antenna voltage of 20 kV had $T_i \sim 3$ eV in the outer SOL, while shots at higher rf power without edge heating had higher SOL ion temperatures. An accurate SOL T_i diagnostic would be needed to test this hypothesis.

The strong temperature dependence of the threshold also sheds light on the observation that edge heating has been observed to start at an H-mode transition. It is reasonable that the decreased transport across the edge during ELM-free H-mode decreases the ion temperature in the SOL, thereby lowering the threshold for PDI. This would explain the increased edge heating that occurs during ELM-free H-mode.

The threshold is independent of the plasma density in the range of interest, as shown in Fig. 8. The threshold increases sharply, though, at densities below 10^{17} m^{-3}, because $\omega_{\rm rf} \sim \omega_{pi}$, which changes the IBW dispersion relation significantly.

3.2.2 Pump wave frequency near a cyclotron harmonic in the SOL

When $\omega_{\rm rf} \simeq \ell\omega_{\rm cD}, \ell = 3, 4\ldots$ in the plasma SOL, the threshold for parametric decay is much lower than it is during H minority heating. There are three effects that contribute to the reduction: the coupling coefficient is larger, the group velocity is slower, and decay into a quasimode and an undamped IBW is possible.

For ion Bernstein waves, $k_\perp \rho_L \gg 1$ at a frequency just above an exact harmonic. This increases the PDI drive term in Eq. 6, because μ is roughly proportional to $k_\perp$ in the regime of interest. Furthermore, the group velocity of the IBW is lower at frequencies just above an exact harmonic, increasing the convective growth $\gamma L/v_g$. These effects have been previously identified as reducing the PDI threshold significantly near harmonics.[17]

On Alcator C-Mod, we have observed edge heating of deuterium during low power ICRF injection in plasmas with $\omega_{\rm rf} \simeq 3\omega_{\rm cD}$ in the plasma edge. The equation for the growth rate is identical to Eq. 6. As in the minority heating regime, the growth rate is limited by damping of the IBW because values of $k_\parallel$ that give significant drive terms through $\mathrm{Im}\,\chi_e(\omega_{\rm ICQM})$ result in IBW damping through $\mathrm{Im}\,\chi_e(\omega_{\rm IBW})$. At the parameters that maximize the growth, ion cyclotron damping of the IBW is negligible.

However, when $\omega_{\rm rf} \simeq 4\omega_{\rm cD}$, parametric decay into an ion cyclotron quasimode at $2\omega_{\rm cD}$ and an IBW just above $2\omega_{\rm cD}$ is also possible. The growth rate is largest at the lowest possible $k_\parallel$, which is restricted by the dominant $k_\parallel$ launched by the antenna and the toroidal width of the pump region. In a cold edge plasma, it is consistent to have

$$\frac{\omega_{\rm IBW}}{k_\parallel v_{te}} \gg 1, \quad \frac{\omega_{\rm IBW} - 2\omega_{\rm cD}}{k_\parallel v_{ti}} \gg 1, \quad \text{and} \quad \omega_q = 2\omega_{\rm cD}, \tag{8}$$

with $\omega_{\rm IBW}$ very close to $2\omega_{\rm cD}$. In this case, the IBW propagates with a relatively slow group velocity, yet is essentially undamped. In a deuterium majority plasma, the PDI growth rate is then approximately

$$\gamma \simeq \frac{|\mu_D - \mu_H|^2}{4\frac{\partial \epsilon_R}{\partial \omega}} \mathrm{Im}\,\chi_H(\omega_{\rm ICQM}). \tag{9}$$

The minimum in the threshold when the resonance is near the edge is shown in Fig. 9. The lowest thresholds in electric field correspond to power levels below 10 kW. Given the low threshold, PDI can be expected to occur over a wide range of plasma parameters when $\omega_{\rm rf} = \ell\omega_{\rm cD}, \ell = 4, 5\ldots$ in the plasma edge.

In the calculations, the PDI is found to be most unstable when $k_\parallel$ of the decay waves was at the lowest allowable value, which is the pump wave $k_\parallel = 22$ m^{-1}. However, this parallel wavelength is sufficiently long that the toroidal field varies significantly over one period, violating the uniform plasma assumption. Restricting $k_\parallel$ to 50 m^{-1} alleviates this problem and raises the threshold in electric field by a factor of 3. As Eq. 9 suggests and is shown in Fig. 9, the threshold is also affected by the percentage of hydrogen in the plasma.

To our knowledge, this solution to the equations has not been included in previous evaluation of PDI.

This result is consistent with our observations of H vs. D edge heating at different harmonics as show in Fig. 4. If $\omega_{\rm rf} = 3\omega_{\rm cD}$ near the edge, decay is into a quasimode at $\omega_{\rm cD}$ and

an IBW damped on electrons near $2\omega_{\rm cD}$. The quasimode damps on deuterium and generates the deuterium tail. When $\omega_{\rm rf} = 4\omega_{\rm cD}$ near the edge, decay is into an undamped IBW and a quasimode at $2\omega_{\rm cD} = \omega_{\rm cH}$ which generates a hydrogen tail.

4 Conclusions

Ideally, one would like to have the opportunity to measure directly the decay modes in front of the rf antenna, specifically their amplitudes, wavelengths, and spatial extent. While direct measurements of the PDI decay waves have been made during lower hybrid heating using laser scattering,[5] similar experiments have not been done during ICRH. The difficulty of this measurement is exacerbated by the small size of the region of the edge in which the decay occurs.

Nevertheless, the agreement between the observations and the theoretical predictions is striking. Specifically, the theoretically predicted and observed thresholds match, including the high power threshold during standard ICRH, the lower threshold when $\omega_{\rm rf} \simeq 3\omega_{\rm cD}$ in the plasma edge, and the lower threshold plus the change from deuterium tails to hydrogen tails when $\omega_{\rm rf} \simeq 4\omega_{\rm cD}$ in the edge. We also have seen theoretically and experimentally that the change in the edge T_i profile at the H-mode transition decreases the PDI threshold.

Given our results it must be assumed the parametric decay will occur over a wide range of parameters and machine configurations in the plasma edge where $\omega_{\rm rf} = \ell\omega_{ci}$. The next step is to address the effect this PDI will have on the plasma performance. The effect depends on the saturation level of the decay, which cannot be calculated as simply as the growth rate. An experiment with direct measurements of the decay waves and an NPA would be perfectly suited to explore the saturation mechanism of the instability and also the relation between the decay wave amplitude and the amplitude and energy distribution of the particle flux. While there is no generation of impurities or loss of heating efficiency due to PDI on Alcator C-Mod, the impact of such instabilities on other machines remains to be examined.

5 Acknowledgements

These results were made possible by the hard work of the engineers, technical staff, and physicists of the Alcator team.

This work was supported by the U.S. Department of Energy Contract No. DE-AC02-78ET51013.

References

[1] I. H. Hutchinson, R. Boivin, F. Bombarda, et al., Phys. Plasmas **1**, 1511 (1994).

[2] M. Porkolab, Fusion Eng. Des. **12**, 93 (1990).

[3] J. C. Reardon, Ph.D. thesis, Massachusetts Institute of Technology, 1999.

[4] J.-M. Noterdaeme and G. Van Oost, Plasma Phys. Control. Fusion **35**, 1481 (1993).

[5] Y. Takase, M. Porkolab, J. J. Schuss, R. L. Watterson, C. L. Fiore, R. E. Slusher, and C. M. Surko, Phys. Fluids **28**, 983 (1985).

[6] J.-M. Noterdaeme, R. Ryter, M. Söll, et al., *13th European Conference on Controlled Fusion and Plasma Heating, Schliersee, 1986*, edited by G. Briffod and M. Kaufmann (European Physical Society, 1986), Vol. 10C(I), p. 137.

[7] F. Wesner, V. M. Prozesky, R. Behrisch, and G. Staudenmaier, Fusion Eng. Des. **12**, 193 (1990).

[8] R. Van Nieuwenhove, G. Van Oost, J.-M. Noterdaeme, M. Brambilla, J. Gernhardt, and M. Porkolab, Nucl. Fusion **28**, 1603 (1988).

[9] G. Van Oost, R. Van Nieuwenhove, R. Koch, et al., Fusion Eng. Des. **12**, 149 (1990).

[10] T. Fujii, M. Saigusa, H. Kimura, et al., Fusion Eng. Des. **12**, 139 (1990).

[11] Y. Takase, R. L. Boivin, F. Bombarda, et al., Plasma Phys. Control. Fusion **38**, 2215 (1996).

[12] B. LaBombard, J. A. Goetz, I. Hutchinson, et al., J. Nucl. Mater. **241-243**, 149 (1997).

[13] A. L. Roquemore, G. Gammel, G. W. Hammett, R. Kaita, and S. S. Medley, Rev. Sci. Instrum. **56**, 1120 (1985).

[14] J. C. Miller, Master's thesis, Massachusetts Institute of Technology, 1995.

[15] R. I. Pinsker, C. C. Petty, M. J. Mayberry, M. Porkolab, and W. W. Heidbrink, Nucl. Fusion **33**, 777 (1993).

[16] M. Porkolab, Phys. Fluids **17**, 1432 (1974).

[17] K. Avinash, W. G. Core, T. Hellston, and C. M. Farrell, The non-resonant decay of the fast magnetosonic wave during ICRH of a tokamak plasma, Technical Report JET-R(88)11, JET Joint Undertaking, 1988.